

Copper complexes of a *p*-phenylenediamine-based bis(tridentate) ligand †

Thomas Buchen,^a Alan Hazell,^b Lars Jessen,^c Christine J. McKenzie,^{*,c} Lars Preuss Nielsen,^c Jens Z. Pedersen^c and Dieter Schollmeyer^a

^a Department of Chemistry, Johannes-Gutenberg-Universität Mainz, Mainz, Germany

^b Department of Chemistry, Aarhus University, 8000 Århus C, Denmark

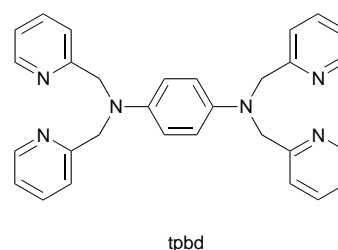
^c Department of Chemistry, Odense University, 5230 Odense M, Denmark

A new bis(tridentate) compound, *N,N,N',N'*-tetrakis(2-pyridylmethyl)benzene-1,4-diamine (tpbd), its diprotonated derivative, $[H_2tpbd]^{2+}$, and a dicopper complex $[Cu_2(tpbd)(H_2O)_4][S_2O_6]_2$ have been prepared and structurally characterized. The pyridyl nitrogen atoms are strongly hydrogen bonded in the crystal structure of the yellow diprotonated salt $tpbd \cdot 2HClO_4 \cdot 2Me_2CO$. The bis(picoyl)amine ends of the ligand show a meridional-type co-ordination to the copper ions in the complex. Magnetic susceptibility measurements on $[Cu_2(tpbd)(H_2O)_4][S_2O_6]_2$ indicate that the *p*-phenylenediamine bridge commutes a weak antiferromagnetic coupling [$J = -15.56(6) \text{ cm}^{-1}$]. Two related dicopper complexes, $Cu_2(tpbd)Cl_4$ and $Cu_2(tpbd)(NO_3)_4$, were also isolated. The ESR spectra of the chloride and nitrate complexes indicated negligible magnetic exchange coupling. Reaction of tpbd with one-electron oxidants generated a purple radical cation which has been characterized by ESR and UV/VIS spectroscopy.

The search for organic building blocks for the construction of dimetallic complexes and one-dimensional co-ordination polymers has led us to investigate tetra-*N*-functionalized *p*-phenylenediamines as potential bis(tridentate) bridging ligands. The strategy was to incorporate each of the two amine nitrogen atoms of the *p*-phenylenediamine unit into the donor set of a tridentate chelating group. Here the new compound *N,N,N',N'*-tetrakis(2-pyridylmethyl)benzene-1,4-diamine (tpbd) and some of its co-ordination chemistry is described.

The electrochemical properties of tpbd's relative, *N,N,N',N'*-tetramethyl-*p*-phenylenediamine (tmpd) are well established.¹ The one-electron oxidation of tmpd gives the radical, Würster's blue cation,¹ which has been isolated in the solid state as a perchlorate,² iodide³ and chloride salt.⁴ The perchlorate salt exhibits a temperature-dependent phase transition with the consequence of altered magnetic properties: paramagnetism at high temperatures and diamagnetism at low.⁵ Conducting compounds based on $tmpd^{+\cdot}$ have been known for some time; the room-temperature conductivity of Würster's blue perchlorate is $10^{-3} \text{ S cm}^{-1}$. Charge-transfer complexes of the type $tmpd^{+\cdot}A^-$ have been also prepared with tmpd as the donor (D^+) and 7,7,8,8-tetracyanoquinodimethane ($tcnq^-$),⁶ pentacyanocyclopentadienyl ($pccp^-$),⁷ tetracyanoplatinate $[Pt(CN)_4]^{2-}$,⁸ bis(maleonitriledithiolato)nickelate(III) $[Ni(mnt)_2]^-$ ⁹ and polyoxomolybdates ($Mo_8O_{26}^{4-}$)¹⁰ as the acceptor (A^-). Thus ligands based on the *p*-phenylenediamine moiety like tpbd have the potential for redox properties which, in conjunction with bound redox-active transition-metal ions, may lead to complexes with both metal ion- and ligand-based redox chemistry.

Our initial investigations into the co-ordination chemistry of tpbd show that monoco-ordinated¹¹ (*i.e.* one end co-ordinated to a metal ion, the other end free), bis-co-ordinated¹¹ (*i.e.* two ligands bound to one metal ion) and bridged (*e.g.* a dinuclear complex with each end of one tpbd bound to a metal ion) complexes can be prepared. This paper describes the latter category of complexes as represented by a series of dicopper complexes, as well as the synthesis and properties of the new compound tpbd. The construction of positively charged one-dimensional co-ordination polymers is conceivable



tpbd

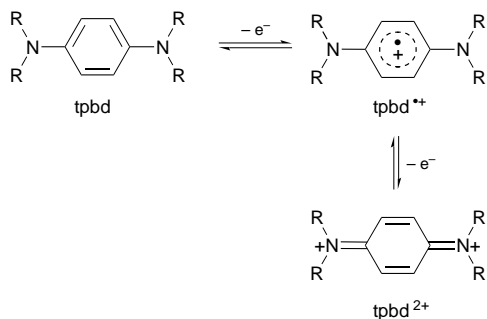
if metal ions with a preference for octahedral geometry are bound by the tridentate ends of two different tpbd ligands, and the tpbd acts as a bridging ligand.

Results and Discussion

Ligand synthesis

The nucleophilic substitution of picoyl chloride [2-(chloromethyl)pyridine] by *p*-phenylenediamine in aqueous solution gives the tetrasubstituted *p*-phenylenediamine derivative, tpbd, as a beige solid product. Reaction times shorter than 14 days led to oily products containing mixtures of the tri-, di- and mono-substituted products. By comparison Sato *et al.*¹² found in their investigations of the substitution reactions of several diamines, that picoyl substitution of *o*-phenylenediamine gives a trisubstituted product with no trace of the anticipated tetrasubstituted product. They did not report any attempt to prepare picoyl-substituted *p*-phenylenediamine derivatives. Given the usual similarities in reactivity of *ortho*- and *para*-substituted benzenes these results might reflect increased steric repulsions in the tetrasubstituted *o*-phenylenediamine product. The compound tpbd is unstable towards an irreversible oxidation process, in solution and in the solid state. Over periods of months its crystals darken. Dark yellow solids are precipitated on the addition of mineral acids to solutions containing tpbd. These products are salts containing the diprotonated tpbd derivative, H_2tpbd^{2+} . The crystal structures of tpbd and $tpbd \cdot 2HClO_4$, see below, show very little difference in corresponding bond lengths of the *p*-phenylenediamine moiety, and both show quinoid character.

† Non-SI unit employed: $G = 10^{-4} \text{ T}$.



Scheme 1 The two-step redox process for tpbd. R = 2-Pyridyl methyl

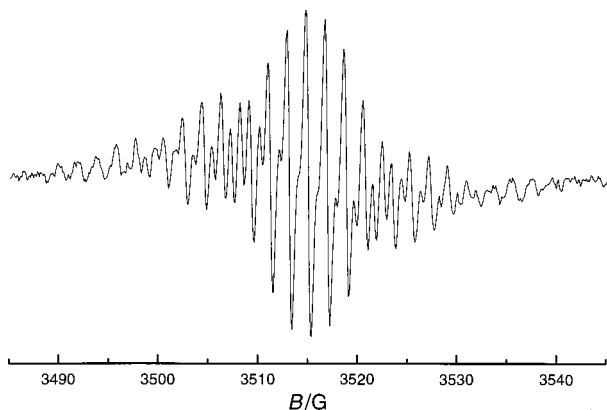


Fig. 1 The ESR spectrum of the radical cation $\text{tpbd}^{\bullet+}$ generated by the oxidation of tpbd by $\text{Fe}(\text{ClO}_4)_3$ in methanol- Me_2SO

The radical cation, $\text{tpbd}^{\bullet+}$

In light of the redox activity of the related tmpd, we have investigated the tendency of tpbd towards oxidation and found that a deep purple radical cation is generated by the oxidation of tpbd by a variety of one-electron oxidants. When $\text{Fe}(\text{ClO}_4)_3 \cdot 6\text{H}_2\text{O}$, $[\text{Mn}_3\text{O}(\text{MeCO}_2)_6]\text{ClO}_4$ or tetrabutylammonium tribromide is added to methanolic solutions of tpbd a purple colour due to the formation of the radical cation $\text{tpbd}^{\bullet+}$ (Scheme 1) develops immediately. The formation and subsequent decay of the $\text{tpbd}^{\bullet+}$ was followed by ESR and UV/VIS spectroscopy. The half-life of this purple cation in methanol at room temperature is approximately 13 min in solutions containing one equivalent of Mn^{3+} ion and approximately 6 min in solutions containing an equivalent of either Fe^{3+} or Br_3^- ion. The ESR spectrum of $\text{tpbd}^{\bullet+}$, generated by one-electron oxidation of tpbd by Fe^{3+} , is shown in Fig. 1. The multi-line signal centred at $g = 2.0031$ indicates that the unpaired electron is delocalized over the 1,4-diaminobenzene moiety. When Mn^{3+} is used as the oxidant a signal for Mn^{2+} grows into the spectrum and the purple colour is more persistent. A possible explanation for the increased stability of $\text{tpbd}^{\bullet+}$ in the presence of Mn^{2+} ions might be stabilization by co-ordination to Mn^{2+} . Intense absorptions at 564 and 612 nm are responsible for the purple colour of the $\text{tpbd}^{\bullet+}$. The UV/VIS spectra of a solution similar to that used for the ESR experiment in Fig. 1 and recorded over 30 min after the addition of the oxidant is shown in Fig. 2. The cyclic voltammogram of tpbd in acetonitrile shows a reversible one-electron redox wave at 310 mV and irreversible oxidation at 670 mV vs. Ag-AgCl. The results from cyclic voltammetry experiments, along with the fact that solutions of tpbd tend to darken, suggest that tpbd is slowly and irreversibly oxidized in solution.

Crystal structures of tpbd and $\text{tpbd} \cdot 2\text{HClO}_4 \cdot 2\text{Me}_2\text{CO}$

The asymmetric unit in the crystal structure of tpbd is shown in Fig. 3. Table 1 lists selected bond distances and angles. The

Table 1 Bond lengths (Å) and angles (°) for tpbd and $\text{tpbd} \cdot 2\text{HClO}_4 \cdot 2\text{Me}_2\text{CO}$

	tpbd	$\text{tpbd} \cdot 2\text{HClO}_4 \cdot 2\text{Me}_2\text{CO}$
N(1)-C(2)	1.446(2)	1.452(4)
N(1)-C(9)	1.445(2)	1.447(5)
N(1)-C(16)	1.391(2)	1.391(4)
C(2)-C(3)	1.514(2)	1.517(4)
C(3)-C(4)	1.380(3)	1.382(5)
C(4)-C(5)	1.377(3)	1.382(6)
C(5)-C(6)	1.376(4)	1.374(6)
C(6)-C(7)	1.359(4)	1.371(5)
C(7)-N(8)	1.336(3)	1.349(4)
C(9)-C(10)	1.509(2)	1.512(5)
C(10)-C(11)	1.383(2)	1.374(5)
C(10)-N(15)	1.338(2)	1.344(4)
C(11)-C(12)	1.377(3)	1.385(6)
C(12)-C(13)	1.374(3)	1.372(6)
C(13)-C(14)	1.366(3)	1.362(6)
C(14)-N(15)	1.338(3)	1.345(5)
C(16)-C(17)	1.403(2)	1.400(4)
C(16)-C(18)	1.402(2)	1.406(5)
C(17)-C(18)	1.380(2)	1.375(5)
C(9)-N(1)-C(2)	119.4(1)	119.5(3)
C(16)-N(1)-C(2)	120.5(1)	119.9(3)
C(16)-N(1)-C(9)	120.0(1)	120.2(3)
N(1)-C(2)-C(3)-N(8)	157.6(2)	-35.7(3)
N(1)-C(9)-C(10)-N(15)	171.5(2)	39.4(3)
C(9)-N(1)-C(16)-C(17)	0.0(2)	0.2(3)

Hydrogen bonds and angles

N(8)-H(8)	0.762(4)
H(8)-N(15)	1.963(4)
N(8)⋯N(15)	2.711(4)
N(15)-H(15)	0.857(4)
N(8)⋯H(15)	1.868(4)
H(8)-N(8)⋯N(15)	167.2(3)
N(15)-H(15)⋯N(8)	167.7(3)

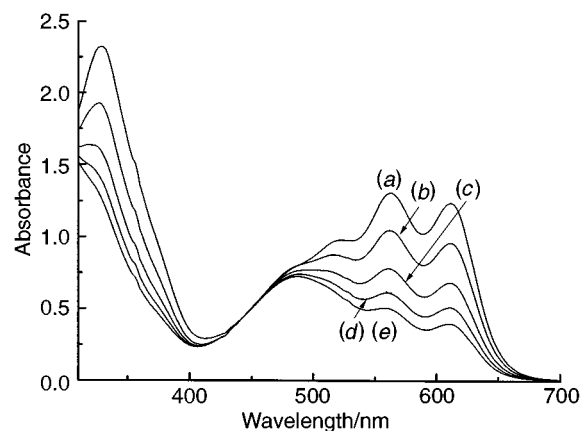


Fig. 2 The UV/VIS spectra of the decay of $\text{tpbd}^{\bullet+}$ in methanol. Spectra recorded after (a) 7, (b) 11, (c) 15, (d) 19 and (e) 23 min. Concentrations of tpbd and $\text{Fe}(\text{ClO}_4)_3$: $350 \mu\text{mol dm}^{-3}$

geometry about the amine nitrogen atoms is relatively planar indicating a π delocalization of the amine nitrogen lone pair with the aromatic system. The three bond angles of N(1) are all very close to 120° . Fig. 4 contains the packing arrangement in the structure of tpbd. The tpbd molecules are interlocked, forming stacks of four pyridine rings, two from each neighbouring molecule. The distances between the rings are 4.91 and 5.85 Å. These distances are greater than those usually attributed to π - π stacking, which may be the result of crystal packing and the fact that four pyridine groups form stacks rather than, for example, the formation of two pairs of more closely associated rings.

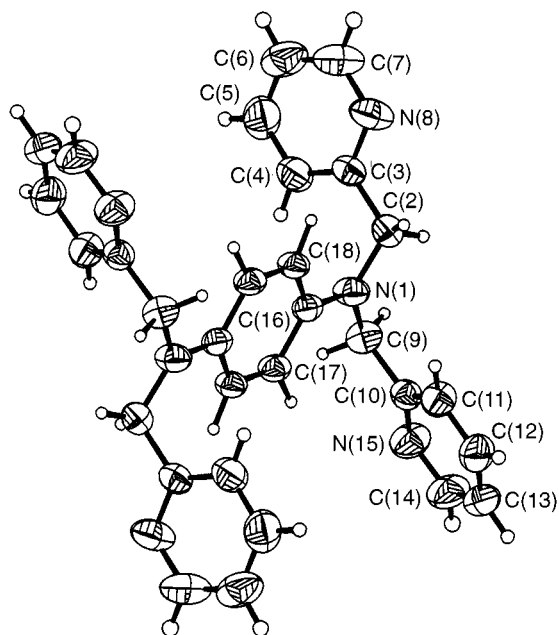


Fig. 3 An ORTEP¹³ plot of tpbd (ellipsoids with 50% probability)

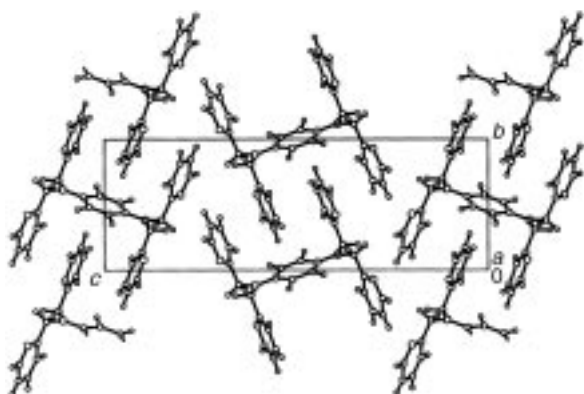


Fig. 4 Packing diagram for tpbd viewed along the *a* axis (PLUTO¹⁴)

The asymmetric unit in the structure of tpbd·2HClO₄·2Me₂CO which contains two perchlorate anions and two molecules of acetone, is shown in Fig. 5. The pyridine N atoms at each end of the molecule are strongly hydrogen bonded by the ionic protons. Each proton is located in two positions with 50% occupancy at each. The interatomic distance between the hydrogen-bonded pyridine nitrogen atoms is 2.711(4) Å. Presumably the reduced base strength of the amine nitrogen atoms due to lone-pair delocalization over the aromatic unit prevents their protonation or hydrogen-bonding involvement. The geometry of the tertiary amine is again planar with bond angles close to 120°.

The bond distances over the phenylenediamine moiety show quinoid character in the structures of both tpbd and [H₂tpbd]²⁺. These distances are very close to the corresponding distances reported for tmpd.² The one-electron and two-electron oxidized forms tmpd^{·+} and tmpd²⁺ have been structurally characterized in salts and the aromatic bond distances in these structures show an only slightly more pronounced quinoid character.^{2a}

Copper complexes

The preparations of three copper(II) complexes are described in the Experimental section. Two are obtained from the reaction of either of CuCl₂·2H₂O or Cu(NO₃)₂·2.5H₂O with tpbd. The third is obtained by hydrolysis of the chloride complex. Two equivalents of copper ions are essential for complex formation;

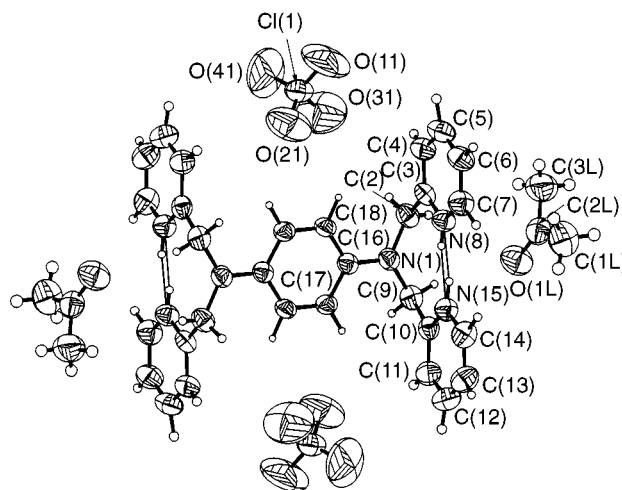


Fig. 5 An ORTEP¹³ plot showing the asymmetric unit of tpbd·2HClO₄·2Me₂CO (ellipsoids with 50% probability)

we have noted that addition of 1 equivalent of Cu²⁺ to solutions containing tpbd gives rise to a transient purple colour most likely due to formation of tpbd^{·+}. Elemental analysis of the microcrystalline green solid chloride complex shows a stoichiometry of tpbd:Cu:Cl=1:2:4. At this stage we believe that an appropriate structural assignment for a complex of this composition is the tpbd-bridged system Cl₂Cu(tpbd)CuCl₂, however we have also considered alternative arrangements, e.g. a dichloride-bridged dicopper complex with one capping monoco-ordinated tpbd, (tpbd)Cu(μ-Cl)₂CuCl₂. The lack of magnetic exchange coupling in Cu₂(tpbd)Cl₄, see below, and the crystal structure of a monoco-ordinated zinc complex [Zn(tpbd)Cl₂]¹¹ lead us to this particular speculation. The second complex in the Experimental section is the tpbd-bridged system, [Cu₂(tpbd)(H₂O)₄][S₂O₆]₂, prepared by the hydrolysis of Cu₂(tpbd)Cl₄. The yield is quantitative without the addition of extra copper ions and with negligible colour remaining in the reaction solution. The aqua complex is a darker green compared to the chloride complex. It is anticipated that tpbd bridges the copper ions also in the nitrate complex, Cu₂(tpbd)(NO₃)₄, however we have not established to what extent the nitrate anions are co-ordinated.

The electrochemical characterization of the copper complexes by cyclic voltammetry was hampered by their general insolubility. It was possible to obtain a rudimentary cyclic voltammogram for [Cu₂(tpbd)(H₂O)₄]⁴⁺, which indicates that oxidation of the ligand is suppressed by co-ordination; no oxidation waves were evident in scanning up to 1 V.

Crystal structure of [Cu₂(tpbd)(H₂O)₄][S₂O₆]₂·MeOH

The cation in [Cu₂(tpbd)(H₂O)₄][S₂O₆]₂·MeOH is shown in Fig. 6. Selected bond distances and angles are listed in Table 2. The tpbd bridges the two copper atoms which are each co-ordinated to three nitrogen atoms and to two water molecules in a distorted square-pyramidal arrangement with Cu–N_{pyridine} 1.978(3) Å, Cu–N_{amine} 2.087(4) Å; the Cu–O(2)(apical) distance of 2.170(5) Å is longer than Cu–O(1)(equatorial) 2.021(4) Å. The complex cation has an exact centre of symmetry. The carbon atom of the methanol of crystallization is disordered over two positions. The copper atoms are located in a *trans* arrangement with respect to the central bridging *p*-phenylenediamine unit. The quinoid character of the linking phenylenediamine unit of [Cu₂(tpbd)(H₂O)₄]⁴⁺ is more pronounced than in tpbd and [H₂tpbd]²⁺ and is consistent with the co-ordination of the amine nitrogen atoms to the electro-positive copper atom. The N_{amine}–C_{aromatic} distance [N(1)–C(1)] is approximately 0.05 Å shorter at 1.461(6) Å than the corresponding distances in free tpbd and its diprotonated salt, 1.391(2) Å. The two pyridine groups at each metal ion show an

Table 2 Selected bond distances (Å) and angles (°) of $[\text{Cu}_2(\text{tpbd})(\text{H}_2\text{O})_4][\text{S}_2\text{O}_6]_2$. Symmetry code I $1 - x, y, 1 - z$

Cu–N(11)	1.973(4)	N(1)–C(27)	1.491(6)
Cu–N(21)	1.982(4)	N(1)–C(17)	1.494(6)
Cu–O(1)	2.021(4)	C(1)–C(3 ¹)	1.385(7)
Cu–N(1)	2.087(4)	C(1)–C(2)	1.400(6)
Cu–O(2)	2.170(5)	C(2)–C(3)	1.375(7)
N(1)–C(1)	1.461(6)		
O(1)–Cu–O(2)	87.5(2)	C(1)–N(1)–C(27)	113.1(4)
O(1)–Cu–N(1)	154.8(2)	C(1)–N(1)–C(17)	111.9(4)
O(1)–Cu–N(11)	97.4(2)	C(17)–N(1)–C(27)	111.3(4)
O(1)–Cu–N(21)	92.9(2)	C(2)–C(1)–C(3 ¹)	118.7(4)
O(2)–Cu–N(1)	117.7(2)	N(1)–C(1)–C(3 ¹)	122.4(4)
O(2)–Cu–N(11)	96.2(2)	N(1)–C(1)–C(2)	118.9(4)
O(2)–Cu–N(21)	95.3(2)	C(1)–C(2)–C(3)	121.2(4)
N(1)–Cu–N(11)	82.9(2)	C(1 ¹)–C(3)–C(2)	120.1(4)
N(1)–Cu–N(21)	83.1(2)	N(1)–C(17)–C(16)	110.8(4)
N(11)–Cu–N(21)	164.9(2)	C(1)–N(1)–C(27)	113.1(4)
Cu–N(1)–C(1)	112.6(3)	C(1)–N(1)–C(17)	111.9(4)
Cu–N(1)–C(17)	106.1(3)	C(17)–N(1)–C(27)	111.3(4)
Cu–N(1)–C(27)	101.2(3)		

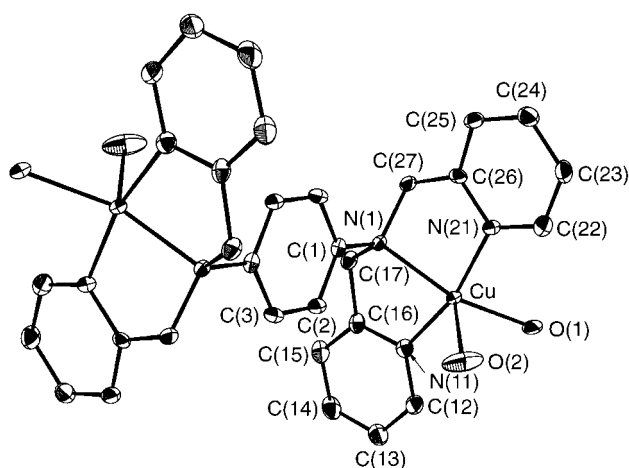


Fig. 6 An ORTEP¹⁵ drawing of the cation in $[\text{Cu}_2(\text{tpbd})(\text{H}_2\text{O})_4][\text{S}_2\text{O}_6]_2$

almost *trans* arrangement with the N(11)–Cu–N(21) angle of 164.9(2)°. A meridional type of co-ordination for the bis(picolyl)amine ends of the ligand is unusual. In contrast, structures of complexes of bis(picolyl)amine and N-substituted bis(picolyl)amine show almost exclusively facial co-ordination of the ligands.¹⁵ As evident in the crystal structures of free tpbd and its diprotonated salt, a rather planar geometry about the tertiary nitrogen atom is the preferred arrangement for this ligand. Hence the essentially meridional co-ordination displayed by tpbd may be a demand of the ligand, due to the clear tendency for delocalization of the aromatic π electrons with the amine nitrogen atoms, rather than ruled by the co-ordinative interaction with the metal ion. A similar meridional arrangement of the tridentate ends, and $N_{\text{amine}}\text{--}C_{\text{aromatic}}$ distance, was observed in the structure of a dicopper complex of a related ligand *p*-phenylenedinitrotetraacetic acid, $[\text{Cu}_2(\text{p-phdta})(\text{H}_2\text{O})_4] \cdot 2\text{H}_2\text{O}$.¹⁶

Magnetic susceptibility

Magnetic susceptibility measurements on $[\text{Cu}_2(\text{tpbd})(\text{H}_2\text{O})_4][\text{S}_2\text{O}_6]_2$ were performed in the temperature range between 5 and 300 K. In Fig. 7 the molar susceptibility is plotted as a function of temperature. It has a maximum value at ca. 15 K and then tends towards zero at very low temperatures (≤ 15 K). This behaviour is typical for antiferromagnetically coupled copper(II) ions. No contribution from paramagnetic impurities was detected at low temperatures.

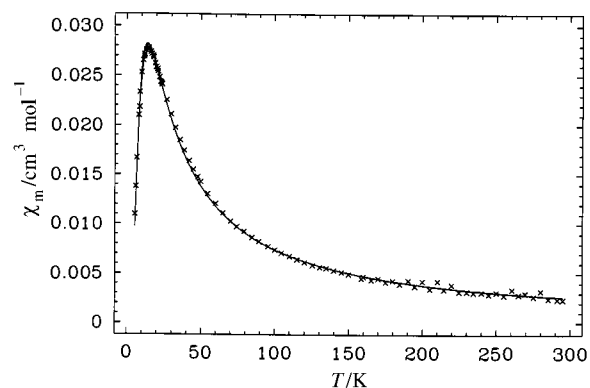


Fig. 7 Plot of magnetic susceptibility vs. temperature for $[\text{Cu}_2(\text{tpbd})(\text{H}_2\text{O})_4][\text{S}_2\text{O}_6]_2$; x, experimental data points

The data were fitted by the Bleaney–Bowers equation¹⁷ (1)

$$\chi = \frac{0.7503g^2}{T[3 + \exp(-J/k_B T)]} \quad (1)$$

using $N_A\beta^2/3k_B = 0.12505$ where g is the averaged g factor, J the coupling constant and k_B the Boltzmann constant. The solid line in Fig. 7 was obtained with $g = 2.046(4)$ and $J = -15.56(6) \text{ cm}^{-1}$. This relatively weak exchange coupling of the unpaired electrons of the copper(II) ions is not entirely unexpected since the superexchange pathway attributed to magnetic exchange coupling interactions is most often described as being *via* the σ -bond framework. In the case of $[\text{Cu}_2(\text{tpbd})(\text{H}_2\text{O})_4][\text{S}_2\text{O}_6]_2$ the pathway is seven bonds long. Weak magnetic coupling has been reported for two other phenylenediamine-bridged dicopper systems. Felthouse and Hendrickson¹⁸ have reported a weak antiferromagnetic exchange interaction of $J = -35 \text{ cm}^{-1}$ for the unsubstituted *p*-phenylenediamine-bridged complex $[(\text{tren})\text{Cu}(\text{pd})\text{Cu}(\text{tren})][\text{NO}_3]_4$ [tren = tris(2-aminoethyl)amine]. Schindler *et al.*¹⁹ have reported some copper complexes of the *meta* homologue of tpbd, *N,N,N',N'*-tetrakis(2-pyridylmethyl)benzene-1,3-diamine (1,3-tpbd). The dinuclear perchlorato-bridged copper(II) complex $[\text{Cu}_2(1,3\text{-tpbd})(\text{ClO}_4)][\text{ClO}_4]_3$ shows by contrast to the present system a weak ferromagnetic coupling with a J of $+10 \text{ cm}^{-1}$.²⁰ A comparison of the magnetic coupling in $[\text{Cu}_2(1,3\text{-tpbd})(\text{ClO}_4)][\text{ClO}_4]_3$ ²⁰ and $[\text{Cu}_2(\text{tpbd})(\text{H}_2\text{O})_4][\text{S}_2\text{O}_6]_2$ is interesting since these complexes appear to demonstrate the spin-polarization mechanism²¹ between paramagnetic ions *via* an aromatic organic bridging group. Ferromagnetism is predicted in cases where there is an odd number of bridging atoms and antiferromagnetism with an even number of bridging atoms. With five atoms between the copper(II) ions of $[\text{Cu}_2(1,3\text{-tpbd})(\text{ClO}_4)][\text{ClO}_4]_3$ the σ framework is one bond shorter than that in $[\text{Cu}_2(\text{tpbd})(\text{H}_2\text{O})_4][\text{S}_2\text{O}_6]_2$. Thus the ferromagnetic and antiferromagnetic exchange coupling observed respectively in these two complexes is expected using this model. The comparison is however complicated by the presence of a second bridging group, the perchlorate ion, between the copper ions in $[\text{Cu}_2(1,3\text{-tpbd})(\text{ClO}_4)][\text{ClO}_4]_3$.

There is no evidence for a magnetic exchange interaction between the copper ions of $\text{Cu}_2(\text{tpbd})\text{Cl}_4$. The data fit Curie–Weiss behaviour with a Weiss constant of 4.5 K. However the plot of χ vs. $1/T$ is not ideal. A possible explanation for this is the presence of an impurity which contributes to the magnetization of the sample to different extents at different temperatures. Trace amounts of the hydrolysis products, in which one or more chloride atoms are replaced by water, are indeed possible.

ESR spectral properties of the copper complexes

The ESR spectrum [solid powdered sample, room temperature

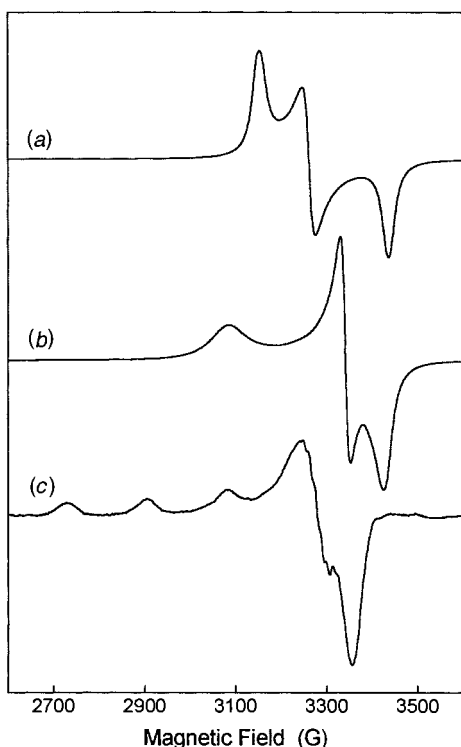


Fig. 8 The ESR spectra of (a) $\text{Cu}(\text{tpbd})\text{Cl}_4$, r.t., solid powdered sample, (b) $[\text{Cu}_2(\text{tpbd})(\text{H}_2\text{O})_4][\text{S}_2\text{O}_6]_2$, r.t., solid powdered sample and (c) $[\text{Cu}_2(\text{tpbd})(\text{H}_2\text{O})_4][\text{S}_2\text{O}_6]_2$, frozen glass in methanol-dmf, -100°C

(r.t.) of $\text{Cu}_2(\text{tpbd})\text{Cl}_4$ shows a rhombic signal with $g_x = 2.034$, $g_y = 2.144$ and $g_z = 2.217$. The presence of only one well defined signal for the chloride complex is indicative of the presence of identical geometrical sites for the copper atoms, and confirms that the electronic distribution about the copper ions is not significantly perturbed by magnetic exchange interactions with neighbouring copper ions. The spectrum of $\text{Cu}_2(\text{tpbd})(\text{NO}_3)_4$ is essentially identical, with $g_x = 2.028$, $g_y = 2.152$ and $g_z = 2.252$. The ESR spectrum of $[\text{Cu}_2(\text{tpbd})(\text{H}_2\text{O})_4][\text{S}_2\text{O}_6]_2$ (solid powdered sample, r.t.) contrasts slightly since the signal shows a tendency towards an axial distortion with $g_x = 2.040$, $g_y = 2.092$ and $g_z = 2.265$. In methanol-dimethylformamide (dmf) solution as a frozen glass the spectrum of $[\text{Cu}_2(\text{tpbd})(\text{H}_2\text{O})_4][\text{S}_2\text{O}_6]_2$ is axial with $g_{\perp} = 2.058$, $g_{\parallel} = 2.248$ and $A_{\parallel} = 176$ G. The solution spectra of $\text{Cu}_2(\text{tpbd})\text{Cl}_4$ and $\text{Cu}_2(\text{tpbd})(\text{NO}_3)_4$ are reminiscent of that for the aqua complex, hence it is likely that the same solution species gives rise to all three spectra as a result of hydrolysis or solvolysis of the terminal ligands in the chloro and nitrate complexes. Fig. 8(a) shows the ESR spectrum of solid $\text{Cu}_2(\text{tpbd})\text{Cl}_4$. Fig. 8(b) and 8(c) show the spectra of $[\text{Cu}_2(\text{tpbd})(\text{H}_2\text{O})_4][\text{S}_2\text{O}_6]_2$ as a powdered solid, and in methanol-dmf solution, respectively. The lack of significant broadening in the ESR signals testifies to negligible magnetic exchange coupling in the dicopper tpbd-bridged complexes which was evident from the magnetic susceptibility measurements.

Experimental

Infrared spectra were measured as KBr discs using a Hitachi 270-30 IR spectrometer, UV/VIS absorption spectra on a Shimadzu UV-3100 spectrophotometer, EI mass spectra on a Varian MAT311A spectrometer and electrospray (ES) ionization mass spectra using a Finnigan TSQ 710 instrument with a combined electrospray and atmospheric pressure chemical ionization source using acetonitrile solutions. NMR spectra were recorded on a Bruker AC 250 spectrometer. Elemental analyses were carried out at the microanalytical laboratory of the H. C. Ørsted Institute, Copenhagen. Electron spin resonance

measurements at X-band frequency were obtained using a Bruker EMX-113 spectrometer. Cyclic voltammograms were measured using a locally constructed three-electrode potentiostat using acetonitrile solutions containing NBu_4PF_6 (0.1 mol dm^{-3}) and a scan rate of 0.100 V s^{-1} . The working electrode was a BAS platinum electrode, the auxiliary electrode was a platinum wire and the reference a BAS Ag-AgCl electrode (calibrant, ferrocene-ferrocenium at 450 mV).

CAUTION: although no problems were encountered in the preparation of the perchlorate salt, suitable care should be taken when handling such potentially hazardous compounds.

Preparations

***N,N,N,N*-Tetrakis(2-pyridylmethyl)benzene-1,4-diamine (tpbd).** A solution of K_2CO_3 (2.81 g, 20.3 mmol) in water (7 cm^3) was slowly added to a vigorously stirred solution of *p*-phenylenediamine (1.61 g, 14.8 mmol) and 2-picoly chloride hydrochloride (11.66 g, 71.2 mmol) in water (7 cm^3). After stirring for 14 d in the dark at room temperature, concentrated NaOH (12 cm^3) was added, resulting in a change from brown to red. After standing at 0°C for several hours the crystalline precipitate was filtered off. Recrystallization from absolute ethanol containing active charcoal yielded the product as beige flakes. Yield 7.018 g, 44.3%; m.p. 206°C (Found: C, 75.65; H, 6.25; N, 17.65. $\text{C}_{30}\text{H}_{28}\text{N}_6$ requires C, 76.25; H, 6.0; N, 17.8%). NMR (CDCl_3) ^1H , δ 4.70 (s, 8 H, CH_2), 6.60 (s, 4 H, C_6H_4), 7.10 (dd, 4 H, py H^5 , $J = 4.2, 7.8$), 7.28 (d, 4 H, py H^3 , $J = 7.8$), 7.57 (t, 4 H, py H^4 , $J = 7.8$) and 8.53 (d, 4 H, py H^6 , $J = 4.2$ Hz); ^{13}C , δ 57.92, 114.33, 121.03, 121.72, 136.51, 140.79, 149.38 and 159.47. IR (KBr, cm^{-1}): 1590, 1528 and 765. ES mass spectrum: m/z 473.2 ($[\text{M} + \text{H}]^+$, 100), 472.2 (M^+ , 30), 381.2 ($[\text{M} + \text{H} - \text{CH}_2\text{C}_5\text{H}_4\text{N}]^+$, 25) and 289.2 ($[\text{M} + \text{H} - 2\text{CH}_2\text{C}_5\text{H}_4\text{N}]^+$, 16%). λ/nm ($\epsilon/\text{dm}^3 \text{ mol}^{-1} \text{ cm}^{-1}$): 341 (566).

***N,N,N,N*-Tetrakis(2-pyridylmethyl)benzene-1,4-diamine dihydroperchlorate, tpbd·2HClO₄.** The compound tpbd (100 mg, 0.212 mmol) was dissolved in a mixture of ethanol (5 cm^3) and water 10 cm^3 . Addition of a few drops of concentrated perchloric acid followed by cooling to r.t. yielded fine yellow crystals, recrystallized from acetone-ethyl acetate. Yield 108 mg (70%) (Found: C, 51.95; H, 4.45; Cl, 10.65; N, 12.5. $\text{C}_{30}\text{H}_{30}\text{Cl}_2\text{N}_6\text{O}_8$ requires C, 53.5; H, 4.5; Cl, 10.55; N, 12.5%). NMR [$(\text{CD}_3)_2\text{SO}$]: δ 4.96 (s, 8 H, CH_2), 6.35 (s, 4 H, C_6H_4), 7.10 (dt, 4 H, py H^5 , $J = 0.7, 6.4$), 7.28 (d, 4 H, py H^3 , $J = 7.9$), 7.57 (dt, 4 H, py H^4 , $J = 7.8, 1.5$) and 8.94 (d, 4 H, py H^6 , $J = 4.7$ Hz); ^{13}C , δ 55.02, 113.45, 123.93, 124.12, 138.05, 142.20, 145.20 and 157.57. IR (KBr, cm^{-1}): 2050 and 1094. ES mass spectrum: m/z 473.2 ($M + \text{H}^+$, 100), 472.2 (M^+ , 80%), 380.2 ($[\text{M} - \text{CH}_2\text{C}_5\text{H}_4\text{N}]^+$, 36) and 237.1 ($[\text{M} + 2\text{H}]^{2+}$, 20%). λ/nm ($\epsilon/\text{dm}^3 \text{ mol}^{-1} \text{ cm}^{-1}$): 333 (2715). X Ray-quality crystals were obtained by diffusion of acetone into an acetonitrile solution of tpbd·2HClO₄.

Tetrachloro[*N,N,N,N*-tetrakis(2-pyridylmethyl)benzene-1,4-diamine]dicopper(II), $\text{Cu}(\text{tpbd})\text{Cl}_4$. Copper(II) chloride dihydrate (71.6 mg, 0.42 mmol) was added to a solution of tpbd (100 mg, 0.21 mmol) in MeOH (20 cm^3). After cooling to room temperature, the product precipitated as a lime-green solid. It was filtered off and washed with methanol, yield 145 mg, 93% (Found: C, 47.0; H, 4.05; Cl, 18.35; N, 10.85. $\text{C}_{30}\text{H}_{32}\text{Cl}_4\text{Cu}_2\text{N}_6$ requires C, 46.35; H, 4.15; Cl, 18.25; N, 10.8%).

Tetraqua[*N,N,N,N*-tetrakis(2-pyridylmethyl)benzene-1,4-diamine]dicopper(II) dithionate, $[\text{Cu}_2(\text{tpbd})(\text{H}_2\text{O})_4][\text{S}_2\text{O}_6]_2 \cdot 3\text{H}_2\text{O}$. The salt $\text{Na}_2\text{S}_2\text{O}_6 \cdot 2\text{H}_2\text{O}$ (86.4 mg, 0.357 mmol) in water (2 cm^3) was added to a solution of $\text{Cu}(\text{tpbd})\text{Cl}_4$ (132.2 mg, 0.1783 mmol) in water (150 cm^3). After 24 h the dark green crystals were filtered off and washed with water, yield 172 mg, 92% (Found: C, 34.3; H, 4.0; N, 7.95; S, 12.15. $\text{C}_{30}\text{H}_{42}\text{Cu}_2\text{N}_6\text{O}_{15}\text{S}_4$ requires C, 33.95; H, 4.0; N, 7.9; S, 12.1%).

Table 3 Crystallographic data and experimental details

	tpbd	tpbd·2HClO ₄ ·2Me ₂ CO	[Cu ₂ (tpbd)(H ₂ O) ₄][S ₂ O ₆] ₂ ·MeOH
Formula	C ₃₀ H ₂₈ N ₆	C ₃₆ H ₄₂ Cl ₂ N ₆ O ₈	C ₃₂ H ₄₄ Cu ₂ N ₆ O ₁₈ S ₄
<i>M</i>	472.58	789.66	1056.06
Crystal system	Monoclinic	Triclinic	Triclinic
Space group	<i>P</i> 2 ₁ / <i>c</i>	<i>P</i> $\bar{1}$	<i>P</i> $\bar{1}$
<i>a</i> /Å	6.2410(5)	8.0672(4)	10.969(4)
<i>b</i> /Å	8.2229(4)	11.1468(3)	8.318(3)
<i>c</i> /Å	24.151(3)	11.4683(3)	10.913(3)
α /°		77.1468(3)	82.61(2)
β /°	93.047(4)	70.772(2)	85.10(2)
γ /°		83.086(2)	89.73(2)
<i>V</i> /Å ³	1237.6(2)	949.37(6)	983.9(6)
Number of reflections centred	25	75	25
<i>T</i> /K	294	294	120
Radiation (λ /Å)	Cu-K α (1.541 78)	Cu-K α (1.541 78)	Mo-K α (0.710 73)
Monochromator	Graphite	Graphite	Graphite
<i>Z</i>	2	1	1
<i>D</i> _c /g cm ⁻³	1.268	1.381	1.782
<i>F</i> (000)	500	414	544
Crystal size/mm	0.06 × 0.35 × 0.54	0.16 × 0.19 × 0.51	0.45 × 0.10 × 0.05
μ (Cu-K α)/mm ⁻¹	0.61	2.09	—
μ (Mo-K α)/mm ⁻¹	—	—	1.371
Absorption correction	No	No	Integration
Transmission factors	—	—	0.870–0.936
Data collection range/°	3 < 2 θ < 150, $\pm h, +k, \pm l$	3 < 2 θ < 150, $+h, \pm k, \pm l$	5 < 2 θ < 56, $+h, \pm k, \pm l$
Decay of standard reflections (%)	5	5	2
No. reflections measured	2545	4186	5277
<i>R</i> _{int}	Not available, <i>N</i> _{obs} = <i>N</i> _{unique}	0.022	0.031
No. unique reflections	2545	3895	4742
No. observed reflections	2122	2926	3022 [<i>I</i> > 3 σ (<i>I</i>)]
No. variables	176	260	291
<i>R</i> ^{<i>a</i>}	0.0496	0.0720	0.051
<i>R</i> ^{<i>b</i>}	0.1555 ^b	0.2313 ^b	0.059 ^c
Goodness of fit	1.044	1.073	1.438
(Δ / σ) _{max}	0.000	0.001	0.007
ρ _{min} , ρ _{max} /e Å ⁻³	0.25, -0.24	0.58, -0.41	-1.4(1), 0.9(1)

^a $R = \sum [|F_o| - |F_c|] / \sum |F_o|$. ^b $R' = \{ \sum [w(F_o^2 - F_c^2)^2] / \sum [w(F_o^2)] \}^{1/2}$, $w = 1 / [\sigma^2(F_o) + (xP)^2 + yP]$; $x, y = 0.0922, 0.22$ for tpbd; 0.1257, 0.60 for tpbd·2HClO₄·2Me₂CO. ^c $R' = \{ \sum w^2 (|F_o| - |F_c|)^2 / \sum w(|F_o|)^2 \}^{1/2}$, $w = 1 / \{ [\sigma_{cs}(F^2) + 1.03F^2]^{1/2} - |F| \}$.

Tetranitrato[*N,N,N,N*-tetrakis(2-pyridylmethyl)benzene-1,4-diamine]dicopper(II), Cu₂(tpbd)(NO₃)₄. Copper(II) nitrate hemipentahydrate (24.6 mg, 0.106 mmol) in MeOH (2 cm³) was added to a solution of tpbd (25 mg, 0.053 mmol) in MeOH (30 cm³). Precipitation of the green product commenced after 5 min. It was filtered off and washed with a small amount of methanol. Yield 35.8 mg, 79.7% (Found: C, 42.25; H, 3.3; N, 15.95. C₃₀H₂₈Cu₂N₁₀O₁₂ requires C, 42.5; H, 3.35; N, 16.5%).

Magnetic studies

Magnetic susceptibilities were measured between 5 and 300 K with a Foner type magnetometer equipped with a helium-flow cryostat. The applied external field was 1 T. The molar susceptibilities were corrected for ligand diamagnetism using Pascal's constants.

X-Ray crystallography

Single crystals of tpbd and tpbd·2HClO₄·2Me₂CO were mounted at 294 K on an Enraf-Nonius CAD4 diffractometer equipped with graphite-monochromated Cu-K α radiation and using the ω -2 θ scan technique. Three standard reflections were monitored every 60 min. A correction for the 5% fall off in intensity observed in both data collections was applied. Crystallographic data and details of structural determinations are listed in Table 3. The structures were solved using direct methods (SIR 92²²). All non H-atoms were refined anisotropically. The H atoms were located in Fourier-difference syntheses and refined isotropically assuming a riding motion model. The refinement was against *F*² (SHELXL 93²³). The two positions of the ionic protons in tpbd·2HClO₄·2Me₂CO were found in

a Fourier-difference map. They were included in the refinement with a fixed site occupation factor of 0.5.

Crystals of [Cu₂(tpbd)(H₂O)₄][S₂O₆]₂·3H₂O suitable for X-ray diffraction studies were isolated directly from the reaction mixture. Intensities were measured using a Huber four-circle diffractometer, at room temperature. Cell dimensions were determined from reflections measured at $\pm 2\theta$. Data were corrected for background, Lorentz-polarization effects, decay and absorption. Crystallographic data and details of structural determinations are listed in Table 3. The structures were determined using SIR 92²² and from subsequent difference electron-density maps and were refined by the minimization of $\sum w(|F_o| - |F_c|)^2$ using a modification of ORFLS.²⁴ Non-hydrogen atoms were refined anisotropically; hydrogen atoms of the ligand were kept at calculated positions (C–H 0.95 Å) with isotropic displacement parameters 20% larger than the equivalent isotropic displacement parameters of the atoms to which they were attached. The refinement was against *F*. For water molecules the hydrogen-atom positions were obtained from difference syntheses where possible but were not refined. Atomic scattering factors and anomalous dispersion corrections were from ref. 25.

Atomic coordinates, thermal parameters, and bond lengths and angles have been deposited at the Cambridge Crystallographic Data Centre (CCDC). See Instructions for Authors, *J. Chem. Soc., Dalton Trans.*, 1997, Issue 1. Any request to the CCDC for this material should quote the full literature citation and the reference number 186/542.

Acknowledgements

Support from the Danish Natural Science Council (grant no. 9503162 to C. J. M.) is acknowledged.

References

- 1 Z. G. Soos and S. R. Bondeson, in *Extended Linear Chain Compounds*, ed. J. S. Millar, Plenum, New York, 1982–1983; vol. 3, pp. 193–261.
- 2 J. L. De Boer and A. Vos, *Acta Crystallogr., Sect. B*, 1972, **28**, (a) 835; (b) 839.
- 3 J. L. De Boer, A. Vos and K. Huml, *Acta Crystallogr., Sect. B*, 1968, **24**, 542.
- 4 A. Mani, B. M. Vedavathi and K. Vijayan, *Curr. Sci.*, 1982, **51**, 192.
- 5 Z. G. Soos and R. C. Hughes, *J. Chem. Phys.*, 1968, **48**, 1066; Z. G. Soos, H. J. Keller, K. Ludolf, J. Queckbörner, D. Wehe and S. Flandrois, *J. Chem. Phys.*, 1981, **74**, 5287.
- 6 A. W. Hanson, *Acta Crystallogr., Sect. B*, 1968, **24**, 768.
- 7 T. P. Radhakrishnan, Z. G. Soos, H. Endres and L. J. Azevedo, *J. Chem. Phys.*, 1986, **85**, 1126.
- 8 H. Endres, W. Jentsch, H. J. Keller, R. Martin, W. Moroni and D. Nöthe, *Z. Naturforsch., Teil B*, 1979, **34**, 140; H. Endres, H. J. Keller, W. Moroni and D. Nöthe, *Inorg. Nucl. Chem. Lett.*, 1976, **12**, 825.
- 9 (a) D. Reefman, J. P. Cornelissen, R. A. G. de Graff, J. G. Haasnoot and J. Reedijk, *Inorg. Chem.*, 1991, **30**, 4928; (b) M. J. Hove, B. M. Hoffman and J. A. Ibers, *J. Chem. Phys.*, 1972, **56**, 3490; (c) B. L. Ramkrishna and P. T. Manoharan, *Inorg. Chem.*, 1983, **22**, 2113.
- 10 D. Attanasio, M. Bonamico, V. Fares and L. Suber, *J. Chem. Soc., Dalton Trans.*, 1992, 2523.
- 11 A. Hazell, C. J. McKenzie and L. P. Nielsen, unpublished work.
- 12 M. Sato, Y. Mori and I. Takeaki, *Synthesis*, 1992, 539.
- 13 C. K. Johnson, ORTEP, ORNL-5138, Revised, Oak Ridge National Laboratory, Oak Ridge, TN, 1976.
- 14 S. Motherwell and W. Clegg, PLUTO 78, Program for Plotting Molecular and Crystal Structures, University of Göttingen, 1978.
- 15 S. Larsen, K. Michelsen and E. Pedersen, *Acta Chem. Scand., Ser. A*, 1986, **40**, 63; J. Glerup, P. A. Goodson, D. J. Hodgson, K. Michelsen, K. M. Nielsen and H. Wiehe, *Inorg. Chem.*, 1992, **31**, 4611; R. J. Butcher and A. W. Addison, *Inorg. Chim. Acta*, 1989, **158**, 211; S. Pal, M. K. Chan and W. H. Armstrong, *J. Am. Chem. Soc.*, 1992, **114**, 6398; S. Pal, M. M. Olmstead and W. H. Armstrong, *Inorg. Chem.*, 1995, **34**, 4708; M. Palaniandavar, T. Pandiyan, M. Lakshminarayanan and H. Manohar, *J. Chem. Soc., Dalton Trans.*, 1995, 455; A. Hazell, K. B. Jensen, C. J. McKenzie, O. Simonsen and H. Toftlund, *Inorg. Chim. Acta*, 1997, **257**, 163.
- 16 C. Ruiz-Pérez, M. L. Rodríguez, F. V. Rodríguez-Romero, A. Mederos, P. Gili and P. Martín-Zarza, *Acta Crystallogr., Sect. C*, 1990, **46**, 1405.
- 17 O. Kahn, *Molecular Magnetism*, VCH, Weinheim, 1993.
- 18 T. R. Felthouse and D. N. Hendrickson, *Inorg. Chem.*, 1978, **17**, 2636.
- 19 S. Schindler, D. Szalda and C. Creutz, *Inorg. Chem.*, 1992, **31**, 2255.
- 20 S. Schindler, personal communication.
- 21 O. Kahn, S. Sikorav, J. Gouteron, S. Jeannin and Y. Jeannin, *Inorg. Chem.*, 1983, **22**, 2877.
- 22 A. Altomare, G. Cascarano, C. Giacovazzo, A. Guagliardi, M. C. Burla, G. Polidori and M. Camalli, SIR 92, a program for automatic solution of crystal structures by direct methods, *J. Appl. Crystallogr.*, 1994, **27**, 435.
- 23 G. M. Sheldrick, SHELXL 93, Program for Crystal Structure Refinement, University of Göttingen, 1993.
- 24 T. Busing, K. O. Martin and H. A. Levy, ORFLS, Report ORNL-TM-305, Oak Ridge National Laboratory, Oak Ridge, TN, 1962.
- 25 *International Tables for X-Ray Crystallography*, Kynoch Press, Birmingham, 1974, vol. 4, p. 72.

Received 6th March 1997; Paper 7/01588G